HHS Public Access

Author manuscript

Mol Cell Neurosci. Author manuscript; available in PMC 2018 March 01.

Published in final edited form as:

Mol Cell Neurosci. 2017 March ; 79: 12–22. doi:10.1016/j.mcn.2016.12.006.

Extracellular vesicles of the blood-brain barrier: role in the HIV-1 associated amyloid beta pathology

Ibolya E. András[1], **Ana Leda**[1], **Marta Garcia Contreras**[2], **Luc Bertrand**[1], **Minseon Park**[1], **Marta Skowronska**[1], and **Michal Toborek**[1]

[1]Department of Biochemistry and Molecular Biology, 1011 NW 15th Street; Gautier Building, Room 528; University of Miami School of Medicine, Miami, FL 33136-1019, USA

[2]Diabetes Research Institute, 1450 NW 10th Ave, University of Miami School of Medicine, Miami, FL 33136-1011, USA

Abstract

HIV-infected brains are characterized by increased amyloid beta (Aβ) deposition. It is believed that the blood-brain barrier (BBB) is critical for Aβ homeostasis and contributes to Aβ accumulation in the brain. Extracellular vesicles (ECV), like exosomes, recently gained a lot of attention as potentially playing a significant role in Aβ pathology. In addition, HIV-1 hijacks the exosomal pathway for budding and release. Therefore, we investigated the involvement of BBB-derived ECV in the HIV-1-induced Aβ pathology in the brain. Our results indicate that HIV-1 increases ECV release from brain endothelial cells as well as elevates their Aβ cargo when compared to controls. Interestingly, brain endothelial cell-derived ECV transferred Aβ to astrocytes and pericytes. Infusion of brain endothelial ECV carrying fluorescent Aβ into the internal carotid artery of mice resulted in Aβ fluorescence associated with brain microvessels and in the brain parenchyma. These results suggest that ECV carrying Aβ can be successfully transferred across the BBB into the brain. Based on these observations, we conclude that HIV-1 facilitates the shedding of brain endothelial ECV carrying Aβ; a process that may increase Aβ exposure of cells of neurovascular unit, and contribute to amyloid deposition in HIV-infected brain.

Keywords

Extracellular vesicles; HIV-1; amyloid beta; blood-brain barrier

Correspondence: Correspondence and requests for materials should be addressed to Michal Toborek or Ibolya E. András: 1011 NW 15th Street; Gautier Building, Room 528; Miami, FL 33136-1019, USA; Phone number: 305-243-0230. mtoborek@med.miami.edu or iandras@med.miami.edu.

INTRODUCTION

Increased amyloid beta (Aβ) deposition is common in the brains of HIV-1 infected individuals (Achim et al. 2009, Brew et al. 2009). It is believed that this process contributes to the development of HIV-associated neurocognitive disorders (HAND), as HAND prevalence in older HIV-1-infected patients is associated with early beta-amyloidosis (Xu and Ikezu 2009, Soontornniyomkij et al. 2012). The most abundant Aβ deposition occurs in the perivascular space, (Green et al. 2005, Xu and Ikezu 2009, Soontornniyomkij et al. 2012, Steinbrink et al. 2013), suggesting that the brain microvessels may be involved in amyloid pathology. In fact, the blood-brain barrier (BBB) is crucial for Aβ homeostasis, and plays a role in Aβ accumulation in the brain (Deane and Zlokovic 2007). To support this notion, we demonstrated that HIV-1 could elevate Aβ levels in human brain endothelial cells (HBMEC), and enhance its transendothelial transfer (Andras et al. 2010, Andras et al. 2012).

Extracellular vesicles (ECV) are heterogeneous in their origin, size, and content. ECV include exosomes with a size of approximately 30–100 nm (Mathivanan et al. 2010), and other larger vesicles (Thery et al. 2009, Meckes and Raab-Traub 2011). Exosomes, are formed in a two-step process involving vesicle budding of the endosomal membranes generating intraendosomal vesicles, followed by the endosome membrane fusion with the plasma membrane which releases these vesicles as exosomes. Their content is diverse and includes mRNAs, miRNAs, lipids and proteins. Exosome cargo can be released into the immediate microenvironment, or at the periphery when exosomes travel via bloodstream. Exosomes being of endosomal origin, contain membrane transport and fusion proteins (e.g., GTPases, annexins, flotillin), tetraspanins (e.g., CD9, CD63, CD81), which are commonly utilized as protein markers for ECV (Vlassov et al. 2012). Exosomes can be taken up into the target cells by endocytosis (Tian et al. 2010).

ECV were recently postulated as having a significant involvement in Aβ pathology, and in various neurodegenerative diseases (Vella et al. 2008, Kalani et al. 2014, Gupta and Pulliam 2014). In addition, HIV-1 is known to use the exosomal pathway to its advantage to generate infectious particles, and to increase viral spread (Sampey et al. 2014). Although ECV released by human brain microvascular cells (HBMEC) were isolated, characterized (Haqqani et al. 2013), and reviewed before (Andras and Toborek 2016), to the best of our knowledge, there are no reports on BBB-derived ECV/exosome involvement in Aβ pathology, especially in the context of HIV-1 infection.

In the present study, we hypothesize that BBB-derived ECV are involved in Aβ transfer into the brain, increasing exposure to Aβ of the BBB-associated cells which form the neurovascular unit. The results indicate that HIV-1 exposure increases the release of ECV from HBMEC, and enhances their loading with Aβ. Interestingly, HBMEC-derived ECV-Aβ cargo can be successfully transferred to astrocytes and pericytes. In addition, infusion of HBMEC-derived ECV with Aβ into the internal carotid artery of mice resulted in association of Aβ with brain microvessels and its delivery into the brain parenchyma.

MATERIALS AND METHODS

Cell cultures

Human brain microvascular endothelial cells (HBMEC) used in the present study represent a stable, well characterized, and differentiated human brain endothelial cell line (Weksler et al. 2005). Briefly, normal human brain endothelial cells were transduced by lentiviral vectors incorporating human telomerase or SV40T antigen. Among several stable immortalized clones obtained by sequential limiting dilution cloning of the transduced cells, the hCMEC/D3 cell line (referred here as HBMEC) was selected as expressing normal endothelial markers and demonstrating blood–brain barrier characteristics. HBMEC for the present study were supplied by Dr. Couraud (Institut Cochin, Paris, France). Cells were cultured on collagen type I (BD Biosciences Pharmingen, San Jose, CA) coated dishes in EBM-2 medium (Clonetics, East Rutherford, NJ) supplemented with VEGF, IGF-1, EGF, basic FGF, hydrocortisone, ascorbate, gentamycin, and 0.5% exosome depleted fetal bovine serum (Exo-FBS; Systems Bioscience, Mountain View, CA).

Human brain astrocytes (SVG astroglia) were purchased from American Type Culture Collection (ATCC, Manassas, VA). They were maintained in Dulbecco's modified Eagle's medium (DMEM; Sigma, St. Louis, MO) supplemented with 10% Exo-FBS (Systems Biosciences), 100 U/ml penicillin, and 100 μg/ml streptomycin at 37°C and 5% CO2.

Human brain pericytes were purchased from ScienCell (Carlsbad, CA) and maintained in Pericyte Medium (ScienCell) supplemented with Pericyte Growth Supplement (PGS, ScienCell), penicillin/streptomycin solution (P/S, ScienCell), and 20% exosome depleted fetal bovine serum (Exo-FBS; Systems Bioscience) at 37°C and 5% CO2.

HIV infection and Aβ treatment

HIV stock was generated using human embryonic kidney (HEK) 293T cells (ATCC) transfected with pYK-JRCSF plasmid containing full-length proviral DNA. Throughout the study, HBMEC were exposed to HIV particles at the p24 level of 30 ng/mL as previously reported (Andras and Toborek 2014). Treatment was terminated by the removal of cell culture media for ECV isolation.

Aβ (1–40) HiLyte was purchased from Anaspec (San Jose, CA). Aβ (1–40) was dissolved in sterile ultra-pure water (ELGA Purelab Classic, Lowell, MA). Freshly solubilized Aβ solutions without pre-aggregation were used for experiments because this form of Aβ was demonstrated to induce proinflammatory reactions in isolated rat brain microvessels (Paris et al. 2002). Aβ (1–40) HiLyte was dissolved first in a basic buffer (0.1 M NH_4OH), and then further diluted in PBS as suggested by the manufacturer. Cells were treated with Aβ (1–40) or Aβ (1–40) HiLyte at the concentration of 100 nM for 48 h in complete medium. Although uptake of Aβ by the BBB occurs rapidly (Yamada et al. 2008), we terminated the treatment at 48 h to allow more ECV to be secreted into the culture medium.

Transfection of brain endothelial cells and ECV isolation

HBMEC were transfected with the CD63 and CD9 Cyto-Tracer constructs (pT CD63-GFP, pT CD9-RFP, respectively) and the non-targeting construct, pT-CYTO RFP (all from Systems Bioscience) using Purefection Transfection Reagent following the manufacturer's protocol. Twenty four hours post transfection, cells were exposed to HIV-1 or/and Aβ (1–40) HiLyte for 48 h.

ECV isolation was performed using ExoQuick-TC exosome precipitation solution (System Bioscience) according to the manufacturer's specifications. Briefly, 10 ml culture medium was mixed thoroughly with 2 ml of Exo-Quick exosome precipitation solution and incubated overnight at 4°C. The next day, samples were centrifuged at 1500 g for 30 min, the supernatant was removed, and centrifuged again at 1500 g for 5 min. The ECV pellet was resuspended in PBS and used for further studies.

ECV infusion surgery

All in vivo experiments were performed according to the guidelines of the American Association for Accreditation of Animal Care (AAALAC), and were approved by the University of Miami Institutional Animal Care and Use Committee. Male C57BL/6 mice of 10 to 12 weeks of age (Jackson Laboratory, Bar Harbor, ME) were weight-matched, and randomly assigned to different treatment groups. Mice were anesthetized with isoflurane, and infused with ECV isolated either from Aβ-exposed HBMEC or saline-treated HBMEC into the brain circulation via the internal carotid artery (ICA), as previously described (Chen et al. 2009). Briefly, the common carotid artery (CCA) was exposed until its bifurcation, where the external carotid artery (ECA) and the ICA begin. Using nylon sutures, a permanent knot was placed at the highest point possible of the ECA, and a removable knot was placed at the lowest point possible of the ECA, immediately above the CCA bifurcation. Next, the CCA and the ICA were temporarily closed using vessel clips. A small incision in the ECA, between the two knots, was performed, where a capillary tubing attached to a syringe containing the ECV solution was inserted. After removing the vessel clip from the ICA, the solution was slowly infused. Mice were euthanized 1 h post infusion, perfused with saline, followed by decapitation, and brain tissue harvesting for microvessel isolation and immunofluorescence, as described below.

Brain microvessel isolation

Brain microvessels were isolated from the ipsilateral hemisphere as previously described, with few modifications (Park et al. 2013). Briefly, dissected brains were homogenized in 4 ml of ice-cold isolation buffer (102.0 mM NaCl, 4.7 mM KCl, 2.5 mM $CaCl_2$, 1.2 mM KH_2PO_4, 1.2 mM $MgSO_4$, 15 mM HEPES, 25 mM $NaHCO_3$, 10 mM glucose, 1 mM Na pyruvate; pH 7.4 with Halt™ protease inhibitor cocktail [Thermo Fisher Scientific, Waltham, MA]). Samples were then filtered through a 300 μm mesh filter (Spectrum Laboratories, Rancho Dominguez, CA), and transferred to a centrifuge tube containing 8 ml of 26% dextran (M.W. 75,000) in isolation buffer solution; followed by centrifugation at 5,800 g, 20 min, at 4°C. After discarding the supernatant, the pellet was resuspended in 2 ml of isolation buffer, filtered through a 120 μm mesh filter (Millipore Sigma, Billerica, MA), and submitted for another round of centrifugation at 1,500 g, for 10 min, at 4°C. The

supernatant was removed, and the pellet was resuspended in 200 μl of isolation buffer. The microvessel-enriched fraction was smeared onto a glass slide (approximately 7 μl per slide), and heat-fixed at 98°C for 10 min.

Slides containing the isolated brain microvessels were washed twice with PBS, incubated for 5 min at room temperature, and stained with DAPI (4',6-Diamidino-2-Phenylindole, Dihydrochloride, Thermo Fisher Scientific) at 1 μg/ml concentration in PBS. Slides were mounted with ProLong Diamond Antifade Mountant (Thermo Fisher Scientific) and imaged on Olympus Fluoview 1200 confocal microscope using a 60× oil immersion lens.

Nanoparticle tracking analysis (NTA)

ECV were analyzed by NanoSight model NS300 (Malvern Instruments Company, Nanosight, Malvern, United Kingdom). Briefly, ECV were isolated from control, HIV-1, and/or Aβ HBMEC cultures. Individual samples were resuspended in 4% paraformaldehyde-PBS and further diluted 100 fold in PBS for analysis. Three 90s videos were recorded for each sample (48 total). The obtained data were analyzed using Nanosight NTA 2.3 Analytical Software (Malvern Instruments Company) with the detection threshold optimized for each sample, and screen gain at 10 in order to track the maximum number of particles with minimal background.

Protein isolation and western blot

Proteins from ECV were extracted with Radio Immuno Precipitation Assay (RIPA) buffer (Pierce, IL, USA) with freshly added protease inhibitors, and 1% Triton-X 100 to inactivate HIV-1. ECV protein concentration was measured by the BCA protein assay kit (Pierce). The proteins (4–8 μg/well) were loaded on sodium dodecyl sulfate polyacrylamide 4–20% ready gels (BioRad, Hercules, CA) and electrotransferred to a nitrocellulose membrane using a transfer pack system (BioRad). The blots were probed with the following primary antibodies overnight at 4°C: rabbit anti-CD9, rabbit anti-CD63, or rabbit anti-HSP70 (1:1,000) in 3% BSA-PBS. Then, the samples were incubated with horseradish peroxidase, conjugated secondary anti-rabbit antibody (1:20,000) in 3% BSA-PBS, for 1 h at room temperature. All primary and secondary antibodies were obtained from System Biosciences. Western blots were washed three times in TBS-T for 10 min after each incubation step. Blots were visualized by means of the ECL Prime Western Blot Detection System (GE Healthcare, Pittsburgh, PA).

Fluorescence microscopy

HBMEC were cultured on collagen I coated chambered glass slides for live cell imaging (ibidi USA, Madison, WI). HBMEC were transfected with pT-CD63-GFP or CD9-RFP for 24 h. Some cultures were cotransfected with CYTO-RFP and CD63-GFP. Cells were then exposed to HIV-1, and live cell imaging was performed 24 h or 48 h post HIV-1 exposure. Selected cultures without transfection were exposed to HIV-1 and/or 100 nM fluorescently labeled Aβ (Aβ HiLyte-Alexa Fluor488). Cell culture media were collected and utilized for ECV isolation. Isolated ECV were placed on glass slides, heated on a heatblock at 95°C for 10 min, and fixed with absolute ethanol for 30 min at 4°C. After being washed with PBS, slides were mounted using ProLong Gold Antifade reagent containing DAPI (Invitrogen,

Carlsbad, CA). Specimens were covered with coverslips, then the immunofluorescent images were captured and evaluated under fluorescence microscopy. Green fluorescence (originating from CD63-GFP or Aβ HiLyte Alexa Fluor488) and red fluorescence (from CD9-RFP) were acquired directly using a Nikon Eclipse Ti-U inverted fluorescence microscope.

Confocal microscopy

Astrocytes treated for 24 h with HBMEC-derived ECV (labeled with CD9-RFP and carrying Aβ (1–40) HiLyte Alexa488) were cultured on chambered glass slides (BD Biosciences, San Jose, CA). After being washed with PBS, the cells were fixed with absolute ethanol for 30 min at 4°C, followed by another wash. The slides were mounted using ProLong Gold Antifade reagent containing DAPI (Invitrogen) to visualize the nuclei. Specimens were covered with coverslips, and the immunofluorescent images were captured and evaluated under confocal microscopy. Red fluorescence originating from endothelial ECV-CD9-RFP, and green fluorescence from ECV-Aβ HiLyte-Alexa Fluor488 were acquired directly through confocal microscopy (Olympus, Fluoview 1200, dry lens UPLFLN 40× NA: 0.75, room temperature), and did not require the use of primary or secondary antibody.

Whole brain tissues were fixed with 4% paraformaldehyde by overnight incubation at 4°C, followed by immersion in a 30% sucrose solution for cryoprotection at 4°C for 48 h. Next, tissues were embedded in Tissue-Tek O.C.T. Compound (Sakura Finetek, Torrance, CA), and frozen in liquid nitrogen. Whole brain tissues were submitted to cryosectioning by means of a cryostat (CryoStar NX70, Thermo Fisher Scientific, Waltham, MA), making 30 μm thick coronal sections that were immersed in a 50% glycerol solution in PBS, and stored at −20°C until the staining procedure.

The floating brain sections were washed three times with PBS, incubated 15 min at room temperature, and permeabilized with 0.2% Triton X-100 (Millipore Sigma, Billerica, MA) in PBS, for 1 h at room temperature. The sections were blocked with 10% normal goat serum (NGS; Abcam, Cambridge, MA), containing 0.1% of NaN_3, overnight at 4°C. The sections were next incubated with anti-CD31 mouse monoclonal, and anti-GFP rabbit polyclonal antibodies (Abcam) at 1:100 dilution in 10% NGS with 0.1% of NaN_3, overnight at 4°C, followed by 6 h incubation at room temperature. Floating sections were washed three times with PBS, incubated 15 min at room temperature, and then overnight at 4°C with goat anti-mouse Alexa Fluor594 or goat anti-rabbit Alexa Fluor488 conjugate secondary antibodies (Thermo Fisher Scientific), at 1:200 dilution in 10% NGS. Afterwards, the sections were washed with PBS, stretched and placed in Superfrost Plus Gold Microscope Slides (Thermo Fisher Scientific). When completely dried, the slides were stained with Hoechst 33342 (Thermo Fisher Scientific) at 1:2,000 dilution in PBS to visualize the nuclei. Slides were mounted with ProLong Diamond Antifade Mountant (Thermo Fisher Scientific) and imaged on Olympus Fluoview 1200 confocal microscope using a 60× oil immersion lens.

Statistical Analysis

Data were analyzed using SigmaPlot for Windows 11.0 software (Systat Software Inc., San Jose, CA). One or two way ANOVA was used to compare responses among treatments.

Treatment means were compared using All Pairwise Multiple Comparison Procedures and $p<0.05$ was considered significant.

RESULTS

Characterization of ECV released from control and HIV-1 exposed brain endothelial cells

Secretion of ECV was traced with CD63-GFP and CD9-RFP fusion Cyto-Tracers by transfecting HBMEC with the pT-CD63-GFP and pT-CD9-RFP constructs, respectively. The tetraspanin CD63 and CD9 are common biomarkers for exosomes. Then, the cells were exposed to HIV-1 particles (30 ng/ml) or vehicle (control) for up to 48 h. Cells transfected with the CD63-GFP or CD9-RFP construct produced green or red (respectively) fluorescent ECV. As demonstrated by live fluorescence microscopy (Figure 1A), CD63-GFP and CD9-RFP positive ECV of different sizes were budding off both control and HIV-infected HBMEC. However, the number of particles budding from HIV-treated HBMEC was visibly greater than in controls. This phenomenon was confirmed by co-transfecting HBMEC with the pT-CYTO-RFP (a non-targeting construct, stains cell cytoplasm, red fluorescence), and pT-CD63-GFP (exosome tracer, green fluorescence) (supplemental Figure 1).

In the next series of experiments, nanoparticle tracking analysis (NTA) was employed to characterize and quantify ECV produced by HBMEC upon exposure to HIV particles or vehicle. The size distribution of control and HIV samples is illustrated in Figure 1B-1D (red error bars in 1B and 1C indicate +/− SEM). ECV originating from control cultures had a mean size of 166.25 nm while the mean size of ECV obtained from HIV-treated cultures was 209.25 nm (Figure 1E).

The isolated ECV were also characterized for exosome marker proteins CD9, CD63, CD81 and Hsp70. The western blot data indicated an increase in protein levels for all of these markers in lysates of ECV originating from HBMEC exposed to HIV-1 particles (Figure 1F), suggesting that HIV-1 may not only increase the number of produced ECV, but also profoundly change the ECV protein profile.

HIV-1 exposure facilitates ECV shedding

To quantify ECV release, HBMEC transiently transfected with pT-CD63 GFP or pT-CD9 RFP were exposed to HIV-1 (30 ng/ml p24) or vehicle for 48 h. The ECV were next isolated from the media of transfected HBMEC, fixed, imaged by fluorescence microscopy, or read in plate reader. Confirming the results from Figure 1A, isolated ECV exhibited different shapes and sizes. The number of CD63 (Figure 2A) and CD9-positive (Figure 2B) ECV in the HIV-1 treated samples was significantly higher as compared to the control samples. The number of GFP or RFP-ECV was normalized to media volume. Subsequent analyses were also performed on the parent cells in which GFP and RFP fluorescence values were normalized to DRAQ5 florescence intensity. While GFP and RFP fluorescence values showed a decreasing tendency in HIV-exposed cells, the changes were not statistically significant (supplemental Figure 2).

While Figure 2A and 2B visualized and quantified only fluorescently-labeled ECV, further analyses by NTA quantified the total number of particles released from control or HIV-1-

exposed HBMEC (Figure 2C). The total ECV number was increased over 5 times (mean 6.242×10^{10} particles/ml) in HIV-1 exposed cultures as compared to controls (mean 1.185×10^{10} particles/ml). Similarly, the number of particles produced by individual cells was significantly higher in HIV-1 treated cultures (~30,000 particles/cell) than in control cells (~7,000 particles/cell) (Figure 2D). Overall, the results in Figures 1 and 2 support the notion that HIV-1 exposure leads to enhanced ECV release from HBMEC.

Exposure to HIV alters Aβ levels in ECV

HIV-1 is known to increase Aβ accumulation and transfer across HBMEC (Andras et al., 2010, 2012); therefore, we evaluated the impact of HIV-1 on Aβ levels in ECV produced by these cells. For these experiments, HBMEC were exposed to HIV-1 (30 ng/ml) and/or 100 nM Aβ (1–40) HiLyte for 48 h, and Aβ (1–40) HiLyte fluorescence was visualized in ECV isolated from cell culture media. Aβ HiLyte was detected in ECV of different sizes both in control, and HIV-1 treated samples (Figure 3A). Consistent with the results presented in Figure 2, there was a visibly higher number of ECV produced by HIV-treated cultures, compared to controls.

Aβ levels in the ECV lysates were next assessed by ELISA and normalized either to cell culture media volume or to ECV protein content (Figures 3B and 3C, respectively). ECV isolated from both control and HIV-treated HBMEC cultures contained Aβ. When normalized to ECV protein levels, these levels were slightly lower in HIV-1-exposed cultures as compared to controls (Figure 3C; left two bars). As expected, exposure to 100 nM Aβ (1–40) HiLyte markedly increased Aβ cargo load in ECV. When normalizing to cell culture volume, Aβ (1–40) levels were significantly higher in the HIV-1 plus Aβ group as compared to the Aβ group (Figure 3B; right two bars). This relationship was reversed, when ECV Aβ levels were normalized to ECV protein levels (Figure 3C; right two bars); presumably because exposure to HIV-1 increased the overall ECV number as demonstrated in Figure 2C. As the result of these changes, Aβ level per vesicle (mean Aβ level divided by the mean ECV number) decreased in HIV-1-treated cultures as compared to respective controls in Figure 3D.

HBMEC-derived ECV transfer their Aβ cargo to recipient neurovascular unit cells

HBMEC form a functional unit with the surrounding pericytes, perivascular astrocytes, microglia, and neurons, called the neurovascular unit (Abbott and Friedman 2012). Therefore, we hypothesized that HBMEC-derived ECV may transfer Aβ to other cells of the neurovascular unit. We tested this notion by implementing astrocytes and pericytes.

HBMEC, transiently transfected with pT-CD9-RFP, were exposed to 100 nM Aβ HiLyte and/or HIV-1 for 48 h, resulting in the secretion of red fluorescent CD9 positive ECV, some of them containing green fluorescent Aβ. ECV were isolated from the cell culture media, and employed for astrocyte or pericyte exposure for 24 h. The colocalization of a green fluorescence signal (corresponding to Aβ HiLyte) with a red fluorescence signal (indicating the HBMEC-derived ECV-CD9-RFP) in the acceptor non-fluorescent astrocytes was assessed by confocal microscopy. Nuclei were stained with DAPI (blue). Figure 4A shows an example of a vesicular structure with overlapping red and green fluorescence present next

to the astrocyte nuclei, indicating an ECV derived from Aβ-treated HBMEC. On a brightfield image this vesicle appears to be still intact. A representative image of astrocyte culture exposed to ECV derived from HIV plus Aβ-treated HBMEC is illustrated in Figure 4B, indicating a variety of vesicular and non-vesicular structures with overlapping red and green fluorescence. Figure 4C visualizes Aβ HiLyte transfer to pericytes by ECV derived from Aβ HiLyte-exposed HBMEC.

ECV-derived Aβ HiLyte fluorescence was next quantified in the recipient astrocytes and pericytes using a plate reader and normalized to DRAQ5 fluorescence (Figure 4D). In astrocytes, a significant fluorescence increase in the recipient astrocytes was observed upon treatment with ECV derived from HIV-1 plus Aβ HiLyte HBMEC compared to Aβ HiLyte alone. These results indicate that transfer of ECV-derived Aβ cargo can be enhanced by HIV-1.

ECV deliver Aβ cargo across the BBB into the brain parenchyma

Following cell culture experiments, we next explored the ability of HBMEC-derived ECV to deliver Aβ across the BBB, and into the brain in vivo. As in previous experiments, HBMEC were transiently transfected with pT-CD63-GFP, and exposed to 100 nM Aβ (1–40) HiLyte (AlexaFluor 647) for 48 h, resulting in the secretion of green fluorescent CD63 positive ECV containing fluorescent Aβ. ECV were isolated from the media, and infused into the internal carotid artery in mice. The delivery method favors the ipsilateral hemisphere for ECV exposure. Control mice were infused with saline. One hour post infusion, the brain microvessels from ipsilateral hemisphere were isolated, and the CD63-GFP positive ECV were identified to be associated with brain capillaries (Figure 5A).

In separate experiments, the brain sections were immunostained with an antibody for the endothelial marker CD31 and with an anti-GFP antibody to better visualize the GFP-labeled ECV marker CD63. The infused ECV containing Aβ were mainly traced to the CD31 positive brain microvessels (Figure 5B, arrows in the enlarged area). However, fluorescent Aβ cargo was also found in the brain tissue, not associated with brain microvessels (Figure 5C, arrowheads in the enlarged area), demonstrating that, indeed, ECV-associated Aβ may be successfully delivered across the BBB into the brain parenchyma.

DISCUSSION

The BBB represents an interface between the circulatory system and the brain tissue, which maintains the homeostasis of the central nervous system. It consists of brain microvascular endothelial cells joined by tight junctions. The surrounding cells, such as pericytes, perivascular astrocytes, microglia, and neurons have a constant modulatory input on the BBB. Working jointly, they constitute a functional entity, called a neurovascular unit. The cells of the neurovascular unit communicate with each other through a complex physiological and pathological cross-talk (Abbott and Friedman 2012). It appears that ECV shed and released by cells of the neurovascular unit may constitute an effective mechanism for intercellular communication. In the present study, we hypothesize that ECV are important in Aβ transfer across the BBB, and amyloid accumulation in the brain of HIV-infected individuals. Although ECV released by HBMEC were isolated, and partially

characterized before (Haqqani et al. 2013), to the best of our knowledge, there are no other reports on BBB-derived ECV involvement in HIV-related Aβ pathology.

There are several methods for ECV isolation, including ExoQuick, ultracentrifugation, or Optiprep. While there is no agreement on a standard isolation procedure, it is important to consider the isolation method used when interpreting reported data (Van Deun et al. 2014). ExoQuick selected in the present study is believed to isolate all ECV, regardless of their size (Quackenbush et al. 2014). This is important since our results indicate that Aβ can be transferred by brain endothelial ECV of various sizes, and they are all likely to be important in Aβ pathology (Andras and Toborek 2016). ECV derived from HIV-exposed culture also tend to be bigger than those produced by control cells. In addition, ExoQuick is regarded as a method to precipitate RNA and protein with greater purity as well as quantity for proteomic analyses, and RNA profiling (Taylor et al. 2011).

The results of the present study indicating the role of ECV in transporting Aβ are consistent with the literature data. It was shown that exosome number increases with aging, and it may be linked to neurodegeneration (Schroer et al. 1992). The first report showing that Aβ can be packaged in exosomes and shed in the microenvironment was published in 2006 (Rajendran et al. 2006). Aβ enclosed in exosomes can contribute to Aβ fibril formation (Yuyama et al. 2008), and to a prion-like propagation of Aβ/Aβ deposits (Vingtdeux et al. 2012). The levels of Aβ 1–42 along with phospho-tau in blood exosomes of neural origin predicted AD up to 10 years before the onset of the disease (Fiandaca et al. 2015).

The exact role of ECV and exosomes in amyloid pathology is not clear (Vella et al. 2008, Kalani et al. 2014, Gupta and Pulliam 2014). It was shown that neuronal exosomes may be protective against Aβ toxicity from being involved in Aβ clearance. For example, neuronal exosomes protected synaptic activity from the harmful effects of Aβ (An et al. 2013). Neuroblastoma-derived exosomes injected into an AD-model mouse brain were shown to take up Aβ and reduce Aβ levels, amyloid depositions, as well as Aβ-mediated synaptotoxicity in the hippocampus (Yuyama et al. 2014, Yuyama et al. 2015). In contrast, an increase in serum exosome levels correlated with an enhanced amyloid plaques in the brains of the 5XFAD mouse model of AD (Dinkins et al. 2015). In additon, reducing exosome secretion by the nSMase2 inhibitor GW4869 resulted in a diminished amount of amyloid plaques in the same mouse model (Dinkins et al. 2014). It was also demonstrated that ECV contain the γ-secretase complex, which potentially results in Aβ synthesis from APP in the vesicles (Sharples et al. 2008). Based on these results, it is believed that exosome Aβ secretion may be protective through the clearance of neurotoxic Aβ; however, secreted exosomes with Aβ cargo can negatively impact other cell types in the microenvironment (Perez-Gonzalez et al. 2012). Exosomes are considered the ‘Trojan horse’ of neurodegenerative diseases, hiding Aβ that can be transferred to other cells (Bellingham et al. 2012). These observations are consistent with the results of the present study in which ECV obtained from HBMEC readily transported Aβ to astrocytes and pericytes. Moreover, infusion of ECV carrying fluorescently labeled Aβ into the internal carotid artery resulted in the association of ECV-Aβ with the brain microvessels, and effective distribution of the fluorescent Aβ cargo into the brain tissue across the BBB.

The ability to load astrocytes with HBMEC-derived Aβ cargo is significant because astrocytes represent an important functional and structural element of the neurovascular unit, as they are essential for the homoeostasis, protection, and regeneration of the brain. Their endfeet surrounding the microvascular endothelium enables a cross-talk between the two cell types and are known to induce the BBB phenotype (Abbott 2002). Astrocytes are the key elements of neuroinflammation (Vartak-Sharma et al. 2014) and Aβ pathology. However, astrocyte responses in the course of neurodegeneration may be diverse even within the same brain. Both reactive astrocytosis and atrophic astrocytes can be observed in AD animal models in early and late stages of the disease (Rodriguez-Arellano et al. 2016). In addition, reactive astroglia remodeling around Aβ deposits and chronic atrophy in Aβ-free regions was described (Verkhratsky et al. 2016). Deposition of Aβ can also induce astrogliosis, oxidative stress, and impaired glutamate uptake by astrocytes (Matos et al. 2008). These alterations can damage the neurovascular unit and contribute to neuronal cell death (Rodriguez et al. 2009).

Besides astrocytes, pericytes also have an important role in Aβ pathology as cells that take part in Aβ clearance. In support of this notion, a greater accumulation of soluble Aβ was observed when pericyte deficient mutant mice were crossed with AD mice overexpressing the Swedish mutation of human APP (Sagare et al. 2013). In addition, Aβ accumulation in pericytes can cause pericyte loss, contributing to neuronal dysfunction (Winkler et al. 2014).

The entry of ECV into recipient cells may involve several mechanisms, such as receptor mediated endocytosis, phagocytosis, and direct fusion with the target cell membrane (Hu et al. 2016). Among these pathways, a receptor-mediated endocytosis via the low-density lipoprotein receptor-related protein 1 (LRP1, CD91) may participate in internalization of brain endothelial ECV-Aβ. Indeed, LRP1 is a receptor for Hsp70 (Basu et al. 2001), a known marker for exosomes, which is also present in ECV derived from HBMEC (Figure 1F). Because LRP1 transports Aβ across the BBB, it is possible that ECV-Aβ cargo triggers this receptors and initiates endocytosis via LRP1-Aβ interaction. This notion is supported by the observations that interaction of exosome-associated Hsp70 with LRP1 results in exosome uptake by dendritic cells (Skokos et al. 2003). This mechanism may potentially be extended to other BBB transporters that commonly transport Aβ, like RAGE. We have shown previously, that exposure to HIV-1 increased RAGE levels in HBMEC, possibly contributing to Aβ accumulation in the brain (Andras et al. 2010). Apart from the exosomal heat-shock proteins, the tetraspanins CD9 and CD81 were also shown play a role in ECV internalization in dendritic cells (Kooijmans et al. 2012). Because these marker proteins are present in HBMEC-derived ECV and their levels robustly increase after HIV-1 exposure (Figure 1F), it is possible that ECV-Aβ cargo delivery may also depend on these proteins.

Interestingly, ECV/exosomes are not only involved in Aβ pathology, but also play an important role in HIV-1 infection (Sampey et al. 2014) (Madison and Okeoma 2015). The exosomal pathway is effectively hijacked by HIV, a process that can contribute to viral spread and increased infectivity. Indeed, exosome-associated HIV-1 particles were shown to be more infectious to the target CD4+ T cells than HIV-1 alone, by a mechanism that might be related to the fact that exo-HIV-1 can hide from the immune system (Wiley and Gummuluru 2006). Exosomes from HIV-1 infected primary human T cells contain high

levels of the trans-activation response element (TAR) RNA, which is important as TAR is required for the trans-activation of the viral promoter and for virus replication. Incubation of these exosomes with primary macrophages caused an increase in proinflammatory cytokines, IL-6 and TNF-beta, possibly through the NF-κB pathway. This phenomenon may be a contributing factor to persistent inflammation observed in HIV-1 infected patients (Sampey et al. 2016).

In light of these observations, it is of utmost importance that HIV-1 exposure markedly increased ECV release from HBMEC as reported in the present study. This phenomenon is not limited to HBMEC as it was shown that monocyte-derived macrophages infected with HIV-1 also secreted ECV in a larger amount (Kadiu et al. 2012). These findings were also confirmed in human samples where both ECV number and size were increased in the plasma of HIV-1 positive ART-naive patients when compared to ART-suppressed patients, elite controllers, or healthy control subjects (Hubert et al. 2015). The mechanism of increased ECV release by HIV-1 may be related to blocking the vesicle tethering by the protein tetherin, a process that can result in the facilitation of vesicle release. Indeed, it was shown that HIV-1 Vpu can antagonize tetherin thus promoting virus budding from the host cell (Pujol et al. 2016).

Exosomes appear to be an important carrier of HIV-1 RNA (Columba Cabezas and Federico 2013) and HIV proteins, such as Gag, Nef (Booth et al. 2006) (Lenassi et al. 2010) or Tat (Rahimian and He 2016), although a recent report questioned the idea that Nef can be transferred intracellularly by exosomes (Luo et al. 2015). Nevertheless, Nef mRNA and Nef protein were found in plasma exosomes of patients with HIV-associated dementia. These exosomes were also able to transfer Nef mRNA to the neuroblastoma cell line SH-SY5Y, leading to Nef protein production in the recipient cells. Importantly, Nef exosomes induced expression and secretion of Aβ (Khan et al. 2016). These observations are consistent with our results, indicating that HIV-1 exposure results in an increase in the overall content of Aβ in ECV, even though this change was not proportional to the overall increase in ECV number.

In summary, our data show that HIV-1 facilitates the shedding of brain endothelial ECV carrying Aβ, which can be transferred to other cell types of the neurovascular unit. When infused into the brain circulatory system, HBMEC-derived ECV carrying Aβ were both associated with the brain microvessels, and found in the brain parenchyma, indicating the crossing of the BBB, and a successful delivery of the ECV-Aβ cargo in vivo. The route may constitute an additional mechanism contributing to brain amyloid accumulation via involvement of the BBB-derived ECV, and the cells of the neurovascular unit. Data from this work contributes to a better understanding of the mechanisms underlying HIV-1-related Aβ pathology in older HIV-1-infected individuals.

Supplementary Material

Refer to Web version on PubMed Central for supplementary material.

Acknowledgments

pYK-JRCSF was obtained from the AIDS Research and Reference Reagent Program, Division of AIDS, NIH/NIAID. Supported by MH098891, MH072567, DA039576, DA027569, HL126559, and by the Miami CFAR MH063022. The content is solely the responsibility of the authors and does not necessarily represent the official views of the National Institutes of Health.

REFERENCES

Abbott NJ. Astrocyte-endothelial interactions and blood-brain barrier permeability. J Anat. 2002; 200(6):629–638. [PubMed: 12162730]

Abbott NJ, Friedman A. Overview and introduction: the blood-brain barrier in health and disease. Epilepsia. 2012; 53(Suppl 6):1–6.

Achim CL, et al. Increased accumulation of intraneuronal amyloid beta in HIV-infected patients. J Neuroimmune Pharmacol. 2009; 4(2):190–199. [PubMed: 19288297]

An K, et al. Exosomes neutralize synaptic-plasticity-disrupting activity of Abeta assemblies in vivo. Mol Brain. 2013; 6:47. [PubMed: 24284042]

Andras IE, et al. HIV-1-induced amyloid beta accumulation in brain endothelial cells is attenuated by simvastatin. Mol Cell Neurosci. 2010; 43(2):232–243. [PubMed: 19944163]

Andras IE, et al. Lipid rafts and functional caveolae regulate HIV-induced amyloid beta accumulation in brain endothelial cells. Biochem Biophys Res Commun. 2012; 421(2):177–183. [PubMed: 22490665]

Andras IE, Toborek M. HIV-1 stimulates nuclear entry of amyloid beta via dynamin dependent EEA1 and TGF-beta/Smad signaling. Exp Cell Res. 2014; 323(1):66–76. [PubMed: 24491918]

Andras IE, Toborek M. Extracellular vesicles of the blood-brain barrier. Tissue Barriers. 2016; 4(1):e1131804. [PubMed: 27141419]

Basu S, et al. CD91 is a common receptor for heat shock proteins gp96, hsp90, hsp70, and calreticulin. Immunity. 2001; 14:303–313. [PubMed: 11290339]

Bellingham SA, et al. Exosomes: vehicles for the transfer of toxic proteins associated with neurodegenerative diseases? Front Physiol. 2012; 3:124. [PubMed: 22563321]

Booth AM, et al. Exosomes and HIV Gag bud from endosome-like domains of the T cell plasma membrane. J Cell Biol. 2006; 172(6):923–935. [PubMed: 16533950]

Brew BJ, et al. Neurodegeneration and ageing in the HAART era. J Neuroimmune Pharmacol. 2009; 4(2):163–174. [PubMed: 19067177]

Chen L, et al. Vessel microport technique for applications in cerebrovascular research. J Neurosci Res. 2009; 87(7):1718–1727. [PubMed: 19115415]

Columba Cabezas S, Federico M. Sequences within RNA coding for HIV-1 Gag p17 are efficiently targeted to exosomes. Cell Microbiol. 2013; 15(3):412–429. [PubMed: 23072732]

Deane R, Zlokovic BV. Role of the blood-brain barrier in the pathogenesis of Alzheimer's disease. Curr Alzheimer Res. 2007; 4(2):191–197. [PubMed: 17430246]

Dinkins MB, et al. Exosome reduction in vivo is associated with lower amyloid plaque load in the 5XFAD mouse model of Alzheimer's disease. Neurobiol Aging. 2014; 35(8):1792–1800. [PubMed: 24650793]

Dinkins MB, et al. The 5XFAD Mouse Model of Alzheimer's Disease Exhibits an Age-Dependent Increase in Anti-Ceramide IgG and Exogenous Administration of Ceramide Further Increases Anti-Ceramide Titers and Amyloid Plaque Burden. J Alzheimers Dis. 2015

Fiandaca MS, et al. Identification of preclinical Alzheimer's disease by a profile of pathogenic proteins in neurally derived blood exosomes: A case-control study. Alzheimers Dement. 2015; 11(6):600–607. e601. [PubMed: 25130657]

Green DA, et al. Brain deposition of beta-amyloid is a common pathologic feature in HIV positive patients. AIDS. 2005; 19(4):407–411. [PubMed: 15750394]

Gupta A, Pulliam L. Exosomes as mediators of neuroinflammation. J Neuroinflammation. 2014; 11:68. [PubMed: 24694258]

Haqqani AS, et al. Method for isolation and molecular characterization of extracellular microvesicles released from brain endothelial cells. Fluids Barriers CNS. 2013; 10(1):4. [PubMed: 23305214]

Hu G, et al. Emerging roles of extracellular vesicles in neurodegenerative disorders: focus on HIV-associated neurological complications. Cell Death Dis. 2016; 7(11):e2481. [PubMed: 27882942]

Hubert A, et al. Elevated Abundance, Size, and MicroRNA Content of Plasma Extracellular Vesicles in Viremic HIV-1+ Patients: Correlations With Known Markers of Disease Progression. J Acquir Immune Defic Syndr. 2015; 70(3):219–227. [PubMed: 26181817]

Kadiu I, et al. Biochemical and biologic characterization of exosomes and microvesicles as facilitators of HIV-1 infection in macrophages. J Immunol. 2012; 189(2):744–754. [PubMed: 22711894]

Kalani A, et al. Exosomes: mediators of neurodegeneration, neuroprotection and therapeutics. Mol Neurobiol. 2014; 49(1):590–600. [PubMed: 23999871]

Khan MB, et al. Nef exosomes isolated from the plasma of individuals with HIV-associated dementia (HAD) can induce Abeta(1–42) secretion in SH-SY5Y neural cells. J Neurovirol. 2016; 22(2): 179–190. [PubMed: 26407718]

Kooijmans SA, et al. Exosome mimetics: a novel class of drug delivery systems. Int J Nanomedicine. 2012; 7:1525–1541. [PubMed: 22619510]

Lenassi M, et al. HIV Nef is secreted in exosomes and triggers apoptosis in bystander CD4+ T cells. Traffic. 2010; 11(1):110–122. [PubMed: 19912576]

Luo X, et al. Exosomes are unlikely involved in intercellular Nef transfer. PLoS One. 2015; 10(4):e0124436. [PubMed: 25919665]

Madison MN, Okeoma CM. Exosomes: Implications in HIV-1 Pathogenesis. Viruses. 2015; 7(7): 4093–4118. [PubMed: 26205405]

Mathivanan S, et al. Exosomes: extracellular organelles important in intercellular communication. J Proteomics. 2010; 73(10):1907–1920. [PubMed: 20601276]

Matos M, et al. Amyloid-beta peptide decreases glutamate uptake in cultured astrocytes: involvement of oxidative stress and mitogen-activated protein kinase cascades. Neuroscience. 2008; 156(4): 898–910. [PubMed: 18790019]

Meckes DG Jr, Raab-Traub N. Microvesicles and viral infection. J Virol. 2011; 85(24):12844–12854. [PubMed: 21976651]

Paris D, et al. Pro-inflammatory effect of freshly solubilized beta-amyloid peptides in the brain. Prostaglandins Other Lipid Mediat. 2002; 70(1–2):1–12. [PubMed: 12428674]

Park M, et al. Methamphetamine-induced occludin endocytosis is mediated by the Arp2/3 complex-regulated actin rearrangement. J Biol Chem. 2013; 288(46):33324–33334. [PubMed: 24081143]

Perez-Gonzalez R, et al. The exosome secretory pathway transports amyloid precursor protein carboxyl-terminal fragments from the cell into the brain extracellular space. J Biol Chem. 2012; 287(51):43108–43115. [PubMed: 23129776]

Pujol FM, et al. HIV-1 Vpu Antagonizes CD317/Tetherin by Adaptor Protein-1-Mediated Exclusion from Virus Assembly Sites. J Virol. 2016; 90(15):6709–6723. [PubMed: 27170757]

Quackenbush JF, et al. Isolation of circulating microRNAs from microvesicles found in human plasma. Methods Mol Biol. 2014; 1102:641–653. [PubMed: 24259003]

Rahimian P, He JJ. Exosome-associated release, uptake, and neurotoxicity of HIV-1 Tat protein. J Neurovirol. 2016

Rajendran L, et al. Alzheimer's disease beta-amyloid peptides are released in association with exosomes. Proc Natl Acad Sci U S A. 2006; 103(30):11172–11177. [PubMed: 16837572]

Rodriguez JJ, et al. Astroglia in dementia and Alzheimer's disease. Cell Death Differ. 2009; 16(3): 378–385. [PubMed: 19057621]

Rodriguez-Arellano JJ, et al. Astrocytes in physiological aging and Alzheimer's disease. Neuroscience. 2016; 323:170–182. [PubMed: 25595973]

Sagare AP, et al. Pericyte loss influences Alzheimer-like neurodegeneration in mice. Nat Commun. 2013; 4:2932. [PubMed: 24336108]

Sampey GC, et al. Exosomes and their role in CNS viral infections. J Neurovirol. 2014; 20(3):199–208. [PubMed: 24578033]

Sampey GC, et al. Exosomes from HIV-1-infected Cells Stimulate Production of Pro-inflammatory Cytokines through Trans-activating Response (TAR) RNA. J Biol Chem. 2016; 291(3):1251–1266. [PubMed: 26553869]

Schroer JA, et al. Fine structure of presynaptic axonal terminals in sympathetic autonomic ganglia of aging and diabetic human subjects. Synapse. 1992; 12(1):1–13. [PubMed: 1411960]

Sharples RA, et al. Inhibition of gamma-secretase causes increased secretion of amyloid precursor protein C-terminal fragments in association with exosomes. FASEB J. 2008; 22(5):1469–1478. [PubMed: 18171695]

Skokos D, et al. Mast cell- derived exosomes induce phenotypic and functional maturation of dendritic cells and elicit specific immune responses in vivo. J Immunol. 2003; 170:3037–3045. [PubMed: 12626558]

Soontornniyomkij V, et al. Cerebral beta-amyloid deposition predicts HIV-associated neurocognitive disorders in APOE epsilon4 carriers. AIDS. 2012; 26(18):2327–2335. [PubMed: 23018443]

Steinbrink F, et al. Cognitive impairment in HIV infection is associated with MRI and CSF pattern of neurodegeneration. Eur J Neurol. 2013; 20(3):420–428. [PubMed: 23095123]

Taylor DD, et al. Exosome isolation for proteomic analyses and RNA profiling. Methods Mol Biol. 2011; 728:235–246. [PubMed: 21468952]

Thery C, et al. Membrane vesicles as conveyors of immune responses. Nat Rev Immunol. 2009; 9(8): 581–593. [PubMed: 19498381]

Tian T, et al. Visualizing of the cellular uptake and intracellular trafficking of exosomes by live-cell microscopy. J Cell Biochem. 2010; 111(2):488–496. [PubMed: 20533300]

Van Deun J, et al. The impact of disparate isolation methods for extracellular vesicles on downstream RNA profiling. J Extracell Vesicles. 2014:3.

Vartak-Sharma N, et al. Astrocyte elevated gene-1 is a novel modulator of HIV-1-associated neuroinflammation via regulation of nuclear factor-kappaB signaling and excitatory amino acid transporter-2 repression. J Biol Chem. 2014; 289(28):19599–19612. [PubMed: 24855648]

Vella LJ, et al. The role of exosomes in the processing of proteins associated with neurodegenerative diseases. Eur Biophys J. 2008; 37(3):323–332. [PubMed: 18064447]

Verkhratsky A, et al. Astroglia dynamics in ageing and Alzheimer's disease. Curr Opin Pharmacol. 2016; 26:74–79. [PubMed: 26515274]

Weksler BB, et al. Blood-brain barrier-specific properties of a human adult brain endothelial cell line. FASEB J. 2005; 19(13):1872–1874. [PubMed: 16141364]

Wiley RD, Gummuluru S. Immature dendritic cell-derived exosomes can mediate HIV-1 trans infection. Proc Natl Acad Sci U S A. 2006; 103(3):738–743. [PubMed: 16407131]

Vingtdeux V, et al. Potential contribution of exosomes to the prion-like propagation of lesions in Alzheimer's disease. Front Physiol. 2012; 3:229. [PubMed: 22783199]

Vlassov AV, et al. Exosomes: current knowledge of their composition, biological functions, and diagnostic and therapeutic potentials. Biochim Biophys Acta. 2012; 1820(7):940–948. [PubMed: 22503788]

Wiley RD, Gummuluru S. Immature dendritic cell-derived exosomes can mediate HIV-1 trans infection. Proc Natl Acad Sci U S A. 2006; 103(3):738–743. [PubMed: 16407131]

Winkler EA, et al. The pericyte: a forgotten cell type with important implications for Alzheimer's disease? Brain Pathol. 2014; 24(4):371–386. [PubMed: 24946075]

Xu J, Ikezu T. The comorbidity of HIV-associated neurocognitive disorders and Alzheimer's disease: a foreseeable medical challenge in post-HAART era. J Neuroimmune Pharmacol. 2009; 4(2):200–212. [PubMed: 19016329]

Yamada K, et al. The low density lipoprotein receptor-related protein 1 mediates uptake of amyloid beta peptides in an in vitro model of the blood-brain barrier cells. J Biol Chem. 2008; 283(50): 34554–34562. [PubMed: 18940800]

Yuyama K, et al. Decreased amyloid-beta pathologies by intracerebral loading of glycosphingolipid-enriched exosomes in Alzheimer model mice. J Biol Chem. 2014; 289(35):24488–24498. [PubMed: 25037226]

Yuyama K, et al. A potential function for neuronal exosomes: sequestering intracerebral amyloid-beta peptide. FEBS Lett. 2015; 589(1):84–88. [PubMed: 25436414]

Highlights

- HIV-1 increases extracellular vesicle (ECV) release from brain endothelial cells
- ECV amyloid beta (Aβ) cargo is elevated by HIV-1
- Brain endothelial cell-derived ECV transfer Aβ to cells of the neurovascular unit
- The described mechanism may contribute to an increase in amyloid deposition in HIV-infected brains

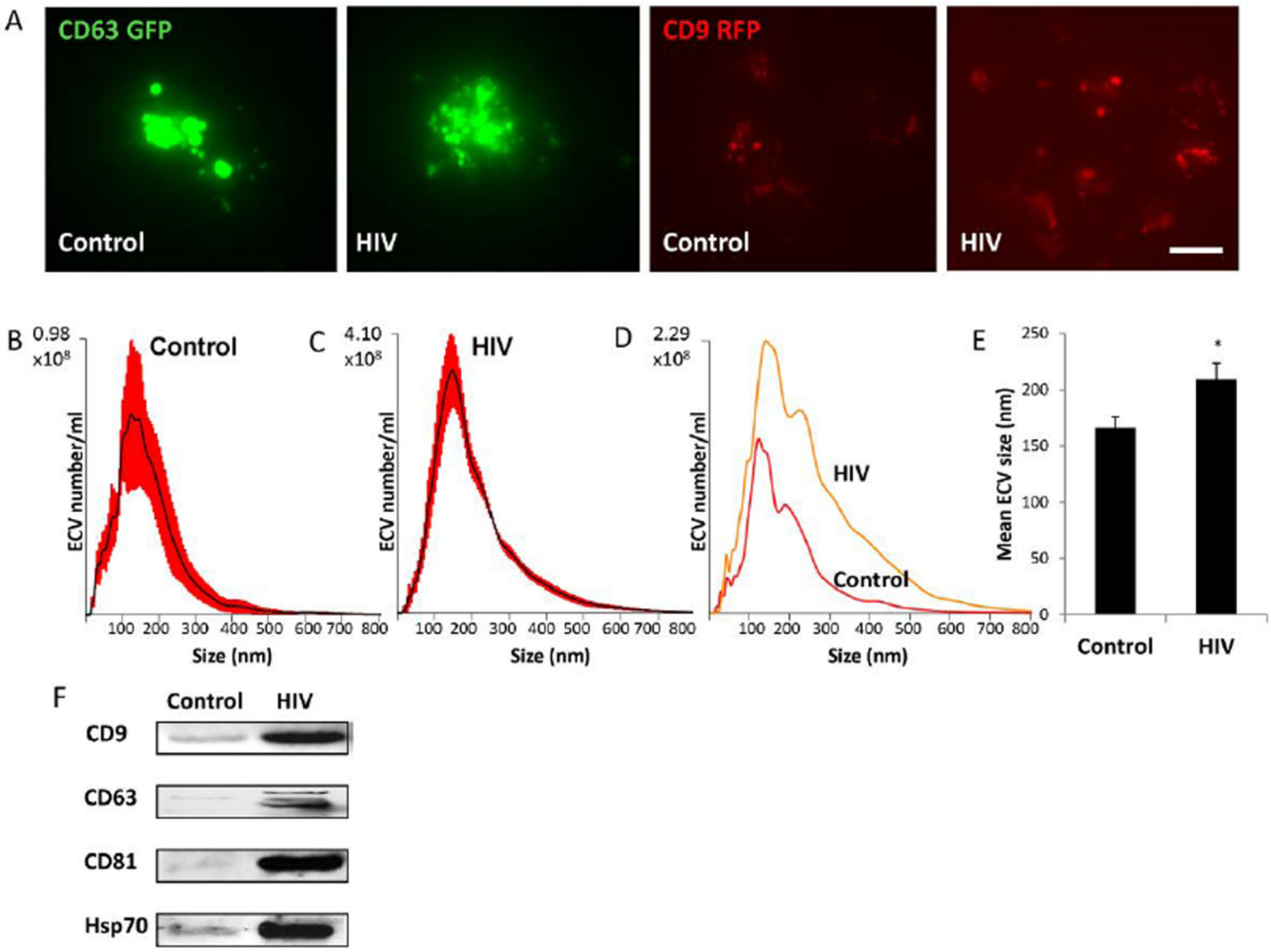

Figure 1. Characterization of extracellular vesicles (ECV) released from control and HIV-1 exposed brain endothelial cells

A) HBMEC were transfected with CD63 or CD9 Cyto-Tracer constructs (pT-CD63-GFP or pT-CD9-RFP), resulting in cells secreting green or red fluorescent ECV. The cells were exposed to 30 ng/ml HIV-1 particles for 48 h. The images represent live imaging of CD63-GFP or CD9-RFP positive ECV budding from control (left panels) and HIV-1 exposed cells (right panels). Scale bar: 20 μm. B and C) Size distribution of isolated ECV (±SEM are represented by red shading, n=4) from control and HIV-treated cultures, respectively. D) A comparison of representative graphs for the control and HIV groups illustrating the differences in size and amount. E) Quantitative analysis of mean ECV size in control and HIV-treated cultures (mean ± SEM, n=4). * Statistically significant as compared to control at $p<0.05$. F) Expression of marker proteins CD9, CD63, CD81, Hsp70 in HBMEC-derived ECV as determined by western blot.

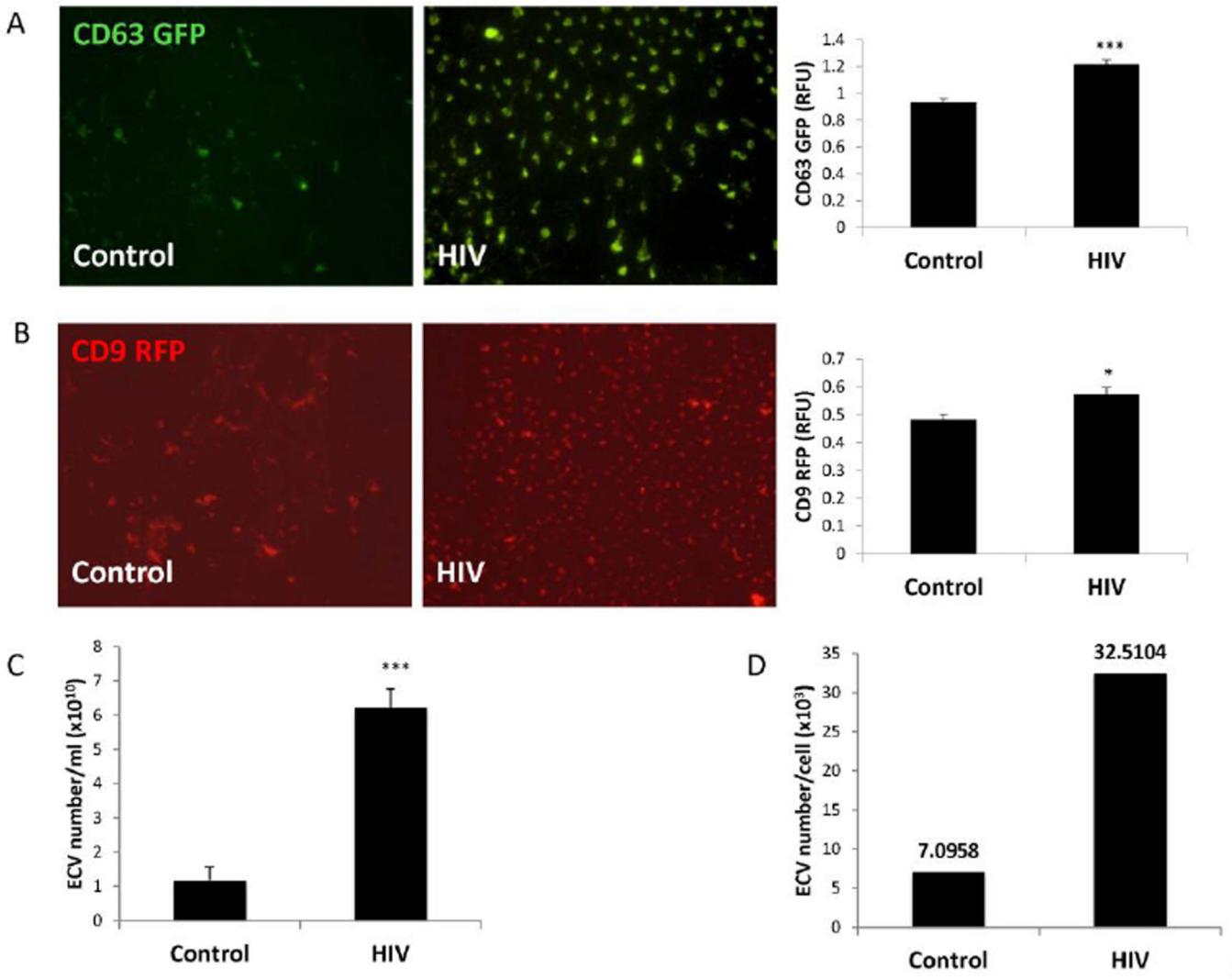

Figure 2. HIV-1 exposure increases brain endothelial ECV secretion

HBMEC were transfected with pT-CD63-GFP (A) or pT-CD9-RFP (B) and exposed to 30 ng/ml HIV-1 for 48 h. Green or red fluorescent ECV were isolated from the culture media, imaged by fluorescence microscopy (scale bar: 20 μm) and quantified using a plate reader. HIV-1 exposure resulted in an increase in CD63-GFP and CD9-RFP positive fluorescence. Values are mean ± SEM, n=14–16. C–D) Non-transected HBMEC were exposed to 30 ng/ml HIV-1 for 48 h, followed by isolation of ECV from the culture media and quantification by NTA. The analyses indicate total ECV number (C) and ECV particle number produced by individual parent cells (D) in control and HIV-1 treated cultures. Values are mean ± SEM, n=4. * Statistically significant as compared to control at $p<0.05$. ***Statistically significant as compared to control at $p<0.001$.

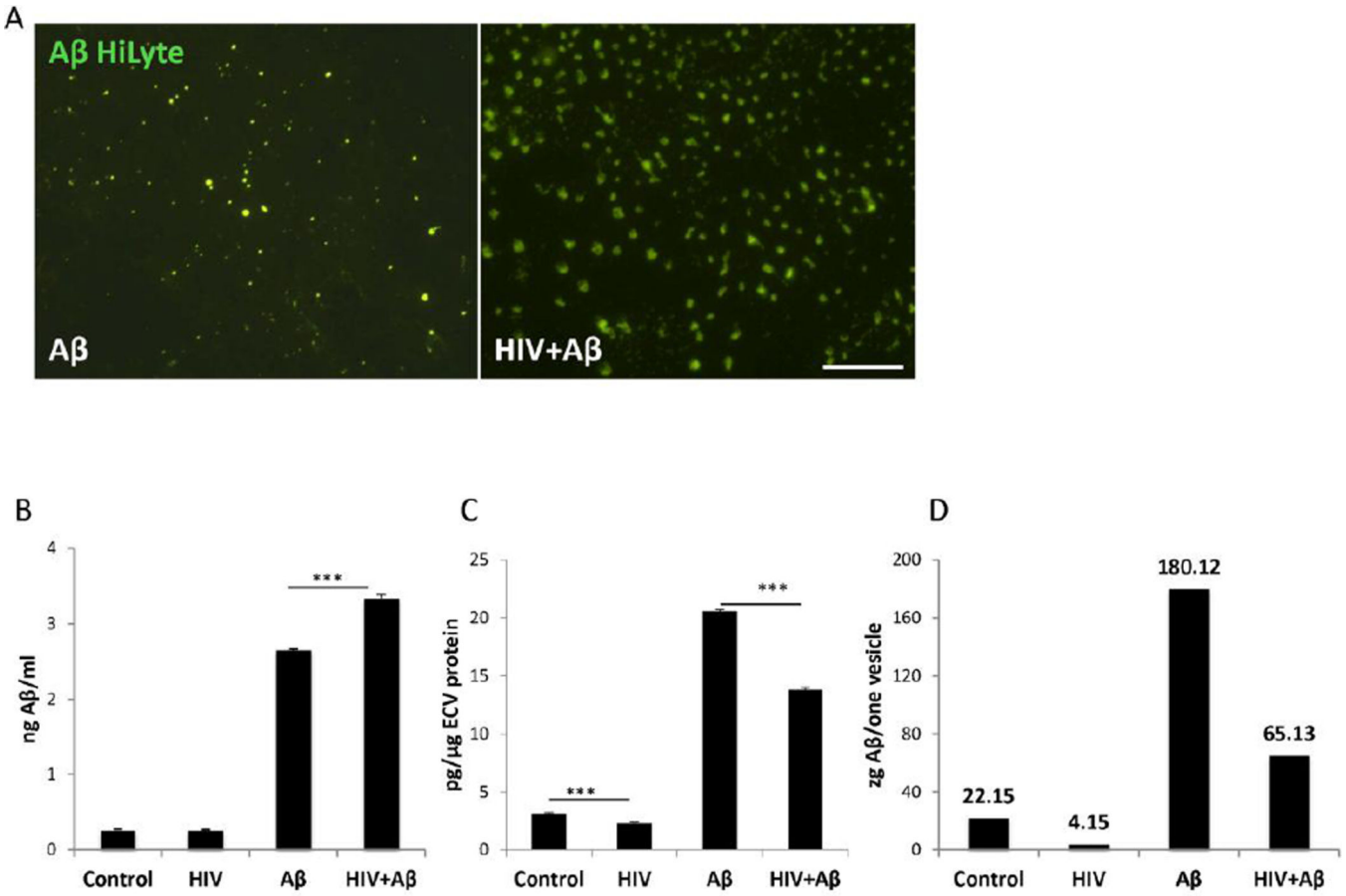

Figure 3. The impact of HIV-1 on Aβ levels in HBMEC-derived ECV

A) Visualization of Aβ (1–40) HiLyte Alexa Fluor488 in ECV isolated from media of HBMEC exposed to HIV (30 ng/ml) and/or 100 nM Aβ (1–40) HiLyte for 48 h. Note different sizes and number of ECV in control and HIV-treated cultures. Aβ (1–40) HiLyte (green fluorescence) was assessed by fluorescence microscopy. Representative images from three experiments. Scale bar: 20 μm. B–C) Aβ (1–40) levels in isolated ECV from media of HBMEC treated as in (A) was measured by ELISA and normalized to cell culture media volume (B) or to ECV protein content (C). D) Aβ (1–40) levels per vesicle (1 zeptogram=10^{-21} g). Values are mean ± SEM, n=4. ***Statistically significant as compared to control or to Aβ (1–40) HiLyte treated group at $p<0.001$.

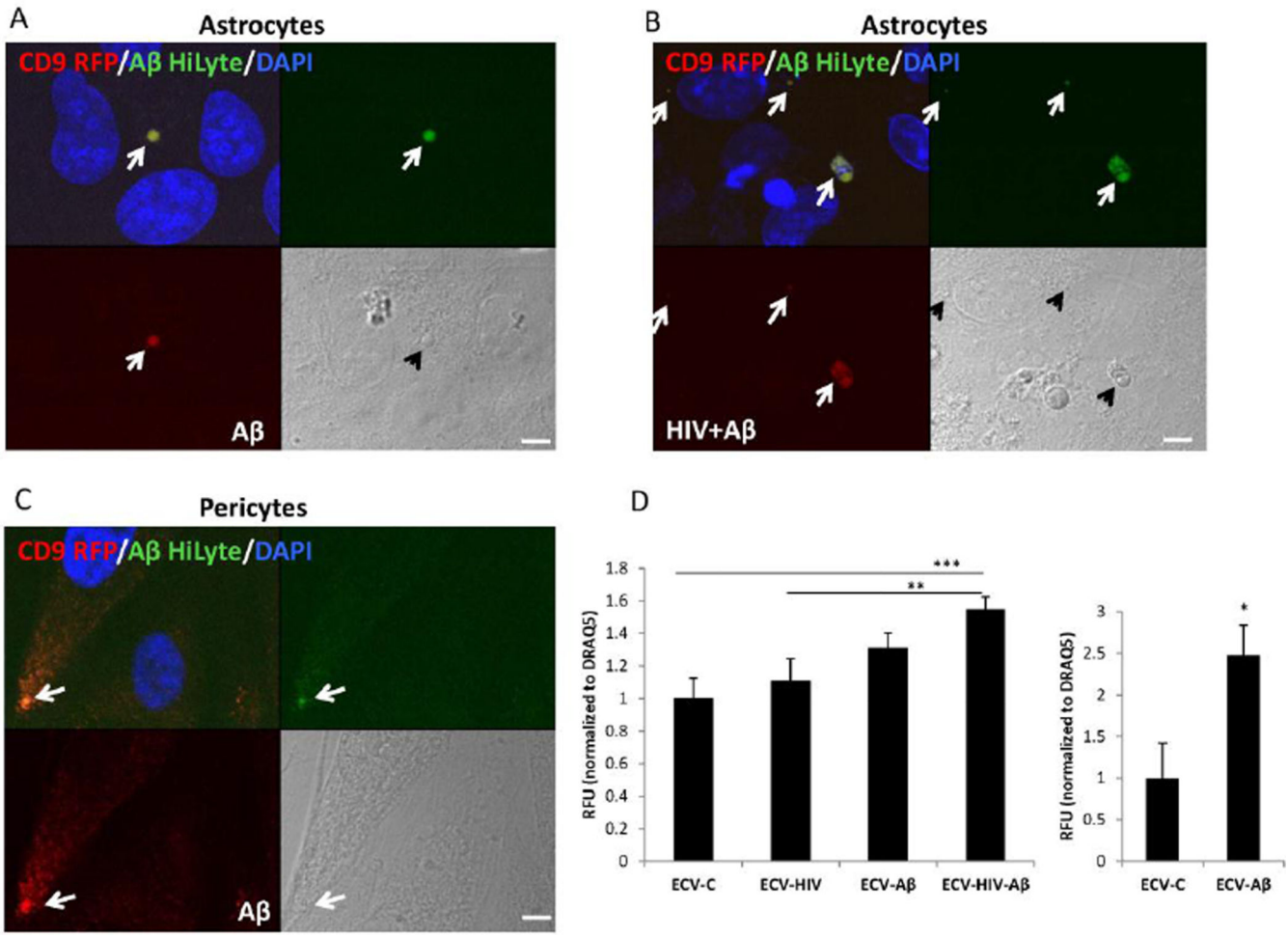

Figure 4. Transfer of Aβ (1–40) HiLyte cargo from donor HBMEC-derived ECV to recipient cells of the neurovascular unit

HBMEC transfected with pT-CD9-RFP were exposed to HIV (30 ng/ml) and/or 100 nM Aβ (1–40) HiLyte Alexa Fluor488 for 48 h, followed by the isolation of ECV from the cell culture media and treatment of astrocytes (A and B) or pericytes (C) for 24 h. All images are performed by confocal microscopy. DAPI staining (blue) visualizes nuclei. Colocalization of CD9-RFP (red fluorescence) and Aβ (1–40) HiLyte (green fluorescence) in astrocytes cultures exposed to ECV from (A) Aβ-treated HBMEC and (B) HIV-1 plus Aβ-treated HBMEC. (C) Colocalization of CD9-RFP (red fluorescence) and Aβ (1–40) HiLyte (green fluorescence) in pericyte cultures exposed to ECV from Aβ-treated HBMEC. Representative images from three experiments. Scale bar: 5 μm. (D) Quantification of Aβ (1–40) HiLyte fluorescence in recipient astrocytes (left graph) and pericytes (right graph). HBMEC were exposed and ECV isolated as in A and B. Astrocytes and pericytes grown on 96-well plates were exposed to fluorescent HBMEC-derived ECV for 24 h. Controls were exposed to non-fluorescent ECV from HBMEC. After washing with PBS, Aβ (1–40) HiLyte fluorescence was measured (abs/em 503/528 nm) in a plate reader. The values were normalized to DRAQ5 fluorescence. Values are mean ± SEM, n=14–16. *Statistically significant as compared to control at $p<0.05$. **Statistically significant as compared to control at $p<0.01$. ***Statistically significant as compared to control at $p<0.001$.

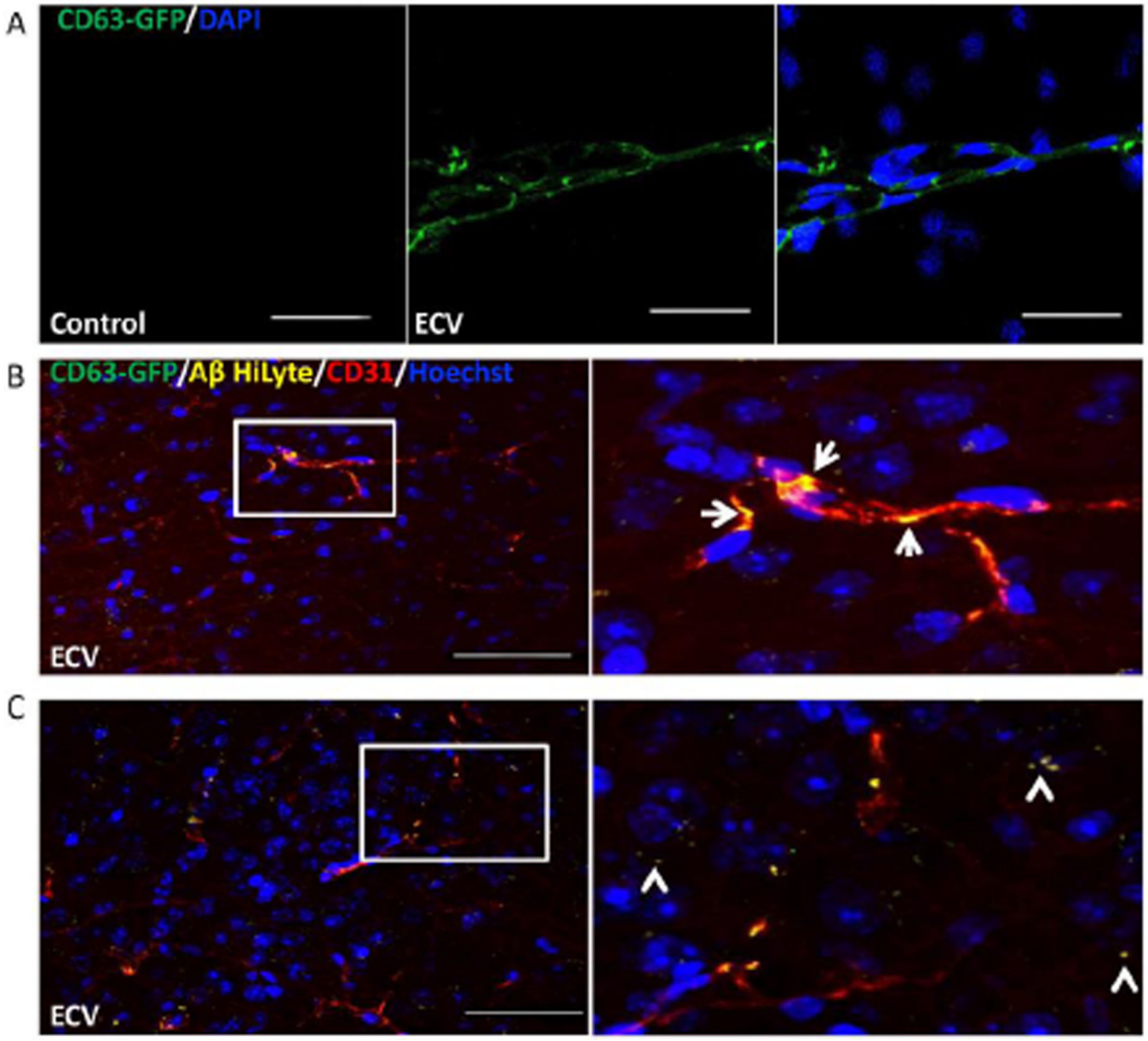

Figure 5. ECV transfer Aβ across the BBB into the brain parenchyma

HBMEC transfected with pT-CD63-GFP were exposed to 100 nM Aβ (1–40) HiLyte AlexaFluor647 for 48 h, followed by isolation of ECV from cell culture media. 2.5×10^7 ECV were infused into the mouse brain via the internal carotid artery. Control mice were infused with saline. Analyses were performed 1 h post infusion by confocal microscopy; DAPI or Hoechst staining (blue) visualizes the nuclei. A) CD63-GFP positive ECV were associated with the isolated brain microvessels. Scale bar: 50 μm. B) Co-localization of CD63-GFP (green), Aβ (1–40) HiLyte AlexaFluor647 (yellow), and CD31 (endothelial marker, red) in the brain sections indicate association of CD63-GFP and Aβ with brain capillaries (arrows on the enlarged right panel). C) Brain sections were analyzed as in (B), indicating partial localization of Aβ in brain parenchyma and not associated with brain

microvessels (arrowheads on the enlarged area), after an apparent crossing the BBB. Scale bar on B and C: 50 μm.

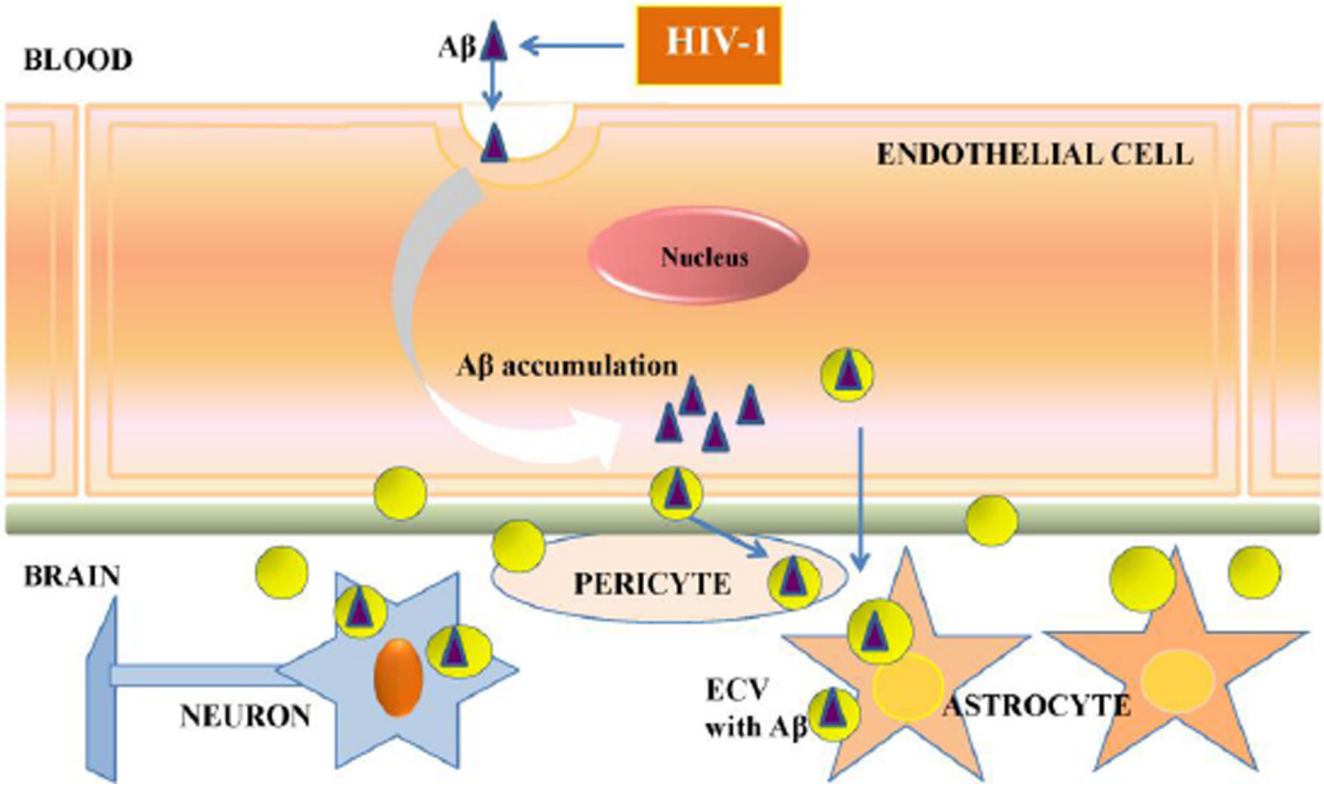

Figure 6. Schematic diagram of the HIV-1 induced Aβ exposure of the neurovascular unit via brain endothelial ECV

Our data indicate that HIV-1 facilitates the shedding of ECV from brain endothelial cells and increases ECV Aβ content. In addition, ECV can transfer Aβ to other cells of neurovascular unit, such as astrocytes and pericytes. These events may contribute to amyloid overload in HIV-infected brain, contributing to the development of neurocognitive dysfunction.

Abbreviations: Aβ, amyloid beta; ECV, extracellular vesicles.